Anal Bioanal Chem (2005) 383: 651–659
DOI 10.1007/s00216-005-0032-7

ORIGINAL PAPER

Cunwang Ge · Wujian Miao · Meiju Ji · Ning Gu

Glutaraldehyde-modified electrode for nonlabeling voltammetric detection of *p16^{INK4A}* gene

Received: 23 April 2005 / Revised: 11 July 2005 / Accepted: 14 July 2005 / Published online: 25 August 2005

Abstract A nonlabeling electrochemical detection method for analyzing the polymerase-chain-reaction-amplified sequence-specific *p16^{INK4A}* gene, in which the basis for the covalent immobilization of deoxyribonucleic acid (DNA) probe is described, has been developed. The self-assembly process was based on the covalent coupling of glutaraldehyde (GA) as an arm molecule onto an amino-functional surface. The *p16^{INK4A}* gene was used as the model target for the methylation detection of early cancer diagnosis. An amino-modified DNA probe was successfully assembled on the GA-coupling surface through the formation of Schiff base under potential control. The hybridization of amino-modified DNA probes with the target was investigated by means of electrochemical measurements, including cyclic voltammetry and square wave voltammetry. Furthermore, the functions of GA coupling for sequence-specific detection were compared with those obtained based on mercaptopropionic acid. Hybridization experiments indicated that the covalent coupling of GA was suitable for the immobilization of DNA probe and was sensitive to the electrochemical detection of single-base mismatches of label-free DNA targets in hybridization. Moreover, reported probe-modified surfaces exhibited excellent stability, and the hybridization reactions were found to be completely reversible and highly specific for recognition in subsequent hybridization processes. The strategy provided the potential for taking full advantage of existing modified electrode technologies and was verified in microarray technology, which could be applied as a useful and powerful tool in electrochemical biosensor and microarray technology.

Keywords DNA hybridization · *p16^{INK4A}* gene · Coupling of glutaraldehyde · Nonlabeling voltammetric detection

C. Ge (✉)
School of Chemistry and Chemical Engineering,
Nantong University,
Nantong 226007, People's Republic of China
e-mail: gecunwang@hotmail.com
Tel.: +86-513-5015895
Fax: +86-513-5015809

C. Ge · M. Ji · N. Gu
Chien-Shiung Wu Laboratory,
Department of Biological Science and Medical Engineering,
Research Center for Nano-scale Science and Technology,
Southeast University,
Nanjing 210096, People's Republic of China

W. Miao
Department of Chemistry and Biochemistry,
The University of Southern Mississippi,
Hattiesburg, MS 39406-5043, USA

Introduction

The *p16^{INK4A}* tumor-suppressor gene participates in establishing and maintaining the malignant phenotypes of a variety of cancer cell lines and primary tumors [1]. The *p16^{INK4A}* gene has been found to be homozygously deleted in cell lines derived from lung, kidney, breast, brain, and skin tumors as well as others, rivaling p53 in the universality of its involvement in tumorigenesis. The *p16* gene promoter contains a 5′-CpG island and is thus a candidate for regulation by deoxyribonucleic acid (DNA) methylation. The under expression or loss of the p16 protein product, even in a cell with a normal intact gene, can lead to failure to inactivate cyclin-D-dependent kinases and, therefore, represents a compromise of regulated cell proliferation [2]. Thus, the detection of aberrant promoter hypermethylation of cancer-related genes could have dramatic effects on the natural history of early cancer diagnosis or the detection of recurrence. Several methods have been developed to evaluate the methylation status of genes, such as Southern blot analysis [3], bisulfite genomic DNA sequencing [4], restriction enzyme polymerase chain reaction (PCR) [5], methylation-specific PCR [6], methylation-sensitive single nucleotide primer extension [7], DNA microarray based on fluorescence or isotope labeling [8, 9], and so on. They have offered useful and powerful tools in studying the phenomenon of DNA methylation. However, the present methods are still laborious, time-consuming, less sensitive, and not rigid enough for clinical applica-

tions. It is of great importance to establish sensitive and reliable methods for the methylation detection of early cancer diagnosis.

The past few years have witnessed an extraordinary surge in interest in developing a DNA electrochemical biosensor for the detection of genes or mutant genes associated with inherited human diseases due to the needs of the Human Genome Project [10]. Combing the technologies in molecular biology, microfabrication, and bioinformatics, electrochemical biosensors offer great hopes for "global views" on DNA variation during biological processes, instead of the traditional gene-by-gene approach, because electrochemical ones provide a simple, rapid, and low-cost point-of-care detection of specific nucleic acid sequences [11, 12]. Early works on DNA hybridization biosensors concentrated on using redox indicators to differentiate between single and double strands of DNA on the electrode. Boon et al. [13] have developed a nonlabeling voltammetric detection method for DNA hybridization by using unlabeled target probes and an electrocatalyst, $[Ru(bpy)3]^{3+}$ (bpy, 2,2′-bipyridine), and by substituting electrochemically inactive inosine for guanosine in capture probes, where catalytic oxidation of guanosine in a target strand provides the signal for hybridization. But only a less than twofold signal from a hybridized electrode has been obtained, compared with the signal from the unhybridized one. In attempts to attain specificity in binding to hybridized electrodes, Takenaka et al. [14] synthesized a threading intercalator with electrochemically active ferrocenes, but they obtained only an approximately fourfold signal difference between the hybridized and unhybridized electrodes. The poor discrimination of hybridized electrodes from unhybridized ones, due to the nonspecific binding of intercalators or metal complexes, has made the practical application of these electrochemical DNA hybridization detection techniques difficult. Moreover, the successful recognition of a specific sequence of DNA requires a highly specific recognition layer. To a large extent, the selectivity and reproducibility of a DNA recognition interface will depend on the immobilization of DNA probe strands. The conformation and packing of the DNA can strongly influence the accessibility of oligonucleotides for hybridization [15]. The probes attached via multiple sites were supposed to have a low reactivity of hybridization. In an ideal system, the probe will be attached to the surface with all the relevant bases freely available for the reaction with an uncoiled target DNA. A high efficiency of the hybridization will be obtained if a DNA probe can be immobilized only on the substrate through the 5′-end or 3′-end position. End point immobilization of the probe strand was achieved by synthesizing a probe with a mercaptohexyl linker at the 5′-end, which was then self-assembled onto the gold electrode by forming thiol–Au bonds. Hybridization efficiency was also improved by preventing the nonspecific adsorption of DNA bases. This was achieved by exposing a probe-modified surface to mercaptohexanol [16, 17] or 2-mercaptoethanol [18]. The strong affinity of the thiol group for gold resulted in the displacement of the less strongly adsorbed bases, thus leaving the DNA attached to the gold only by the end point thiol group. But the preparation of functional mercapto-DNA is very labor-intensive. The procedure for the modification of DNA is rather complicated and unreliable because of a tendency toward oxidative dimerization to form disulfide, and a reducer may need to be added for DNA immobilization [19]. The labeling of the target is not only time-consuming and rather expansive, but also changes the level originally presented in the sample.

In the present paper, our experiments are largely based on the precept that an improved surface chemistry can lead to improved sensitivity and selectivity in DNA hybridization. The basis for immobilization of DNA probes through glutaraldehyde (GA) coupling was verified for the nonlabeling voltammetric detection of the $p16^{INK4A}$ gene based on our previously reported potential control immobilization [20] and microarray used to analyze the methylation patterns of $p16^{INK4A}$ [9]. To our knowledge, the covalent coupling of GA, which is a conventional approach to the coupling of proteins, has not been reported in the attachment of an amino-modified DNA on modified electrodes until now. It allows one to work with label-free targets, to minimize background signals, and to attain a large discrimination of one-base mismatches in the voltammetric detection of DNA hybridization. The function of the basis of GA was compared with that obtained based on mercaptopropionic acid (MPA) coupling. In addition, the current probe-modified surfaces are stable, and hybridization reactions are found to be completely reversible and specific in a series of experiments. The results indicate that this approach for the immobilization of DNA is suitable for the electrochemical detection of label-free DNA targets and in microarray analyses.

Materials and methods

Materials

DNA probes and targets used were specially designed according to the $p16^{INK4A}$ gene (GenBank accession no. AH005371) to determine the methylation status of the CpG sites of the *p16* gene, which was processed by bisulfite. All amino-modified $p16^{INK4A}$ DNA probes and PCR-amplified targets were synthesized and purified by Shenyou (Shanghai, China). The amino-modified probes, oligonucleotides, and targets had the following sequences:Probe, Complementary, 5′-NH_2-GCC GCC CGC TAC CTA-3′ (p1); One-base mismatch, 5′-NH_2-GCC GCC CAC TAC CTA-3′ (p2); Noncomplementary, 5′-NH_2-AAC GCA CAC AAT CCA-3′ (p3); Target, 3′-GAT CGG CGG GCG ATG GAT TTA-5′ (t1).

The manufacturer provided the value of optical density corresponding to the strand amount for each oligonucleotide. Each oligonucleotide was dissolved in an adequate volume of sterilized water to prepare a stock solution of 10 μg ml^{-1} strand concentration. The target for microarray was labeled with Cy3 fluorescein on the 5′-end with the same target sequence above. GA (50% water solution;

Amresco), 2-aminoethanethiol (AET; Sigma), MPA (Sigma), 1-ethyl-3(3-dimethyl-aminopropyl)-carbodiimide (EDC; Sigma), and *N*-hydroxysulfo-succinimide (NHS; Acros) were used without further purification. $[Co(phen)_3](ClO_4)_3$ was prepared according to the literature [21]. The following buffers were involved in the study: 0.1 mol l^{-1} phosphate-buffered saline (PBS; 0.1 mol l^{-1} NaCl+ 10 mmol l^{-1} sodium phosphate buffer, pH 7.4), Tris–HCl buffer (5 mM Tris–HCl and 50 mM NaCl, pH 7.1), TE buffer (10 mmol l^{-1} Tris–HCl+1.0 mmol l^{-1} ethylenediaminetetraacetic acid, pH 8.0), and 2× SSC–0.1% sodium dodecyl sulfate (SDS) buffer (300 mmol l^{-1} sodium chloride/30 mmol l^{-1} sodium citrate/0.1% SDS, pH 7.0). All other reagents used were of analytical purity. Millipore water was predistilled twice and sterilized in Milli-Q plus (Millipore, Bedford, MA).

Apparatus

Electrochemical measurements were performed on a CHI 660A workstation (CH Instrument, Austin, TX). The electrochemical cell consisted of a three-electrode system, with a gold or modified gold disk electrode (2.0 mm in diameter, CHI 101; CH Instrument) as the working electrode, a saturated calomel electrode (SCE) as the reference electrode, and a platinum flag as the auxiliary electrode, respectively. All solutions were deaerated with high-purity nitrogen and kept under a nitrogen atmosphere throughout the electrochemical measurements. All reported current intensities were averaged for three parallel experiments. All reported potentials were against the SCE. The binding of the DNA redox species with the probe or probe–target hybrid on the gold surface took place in the 0.12 mM $[Co(phen)_3](ClO_4)_3$ solution (in Tris–HCl buffer, pH 7.1). After immersion for 10 min, the electrode was measured by cyclic voltammetry (CV) and square wave voltammetry (SWV), with a square wave amplitude of 25 mV and a square wave frequency of 30 Hz. The experimental temperature of CV and SWV was controlled at 25±1°C. All measurements, unless specified otherwise, were the averages of at least three to five replicated measurements.

Procedure

Single-stranded DNA probe immobilization on GA-modified electrode

Gold electrodes were used throughout the electrochemical measurements. A gold electrode modified with AET abounded with amino groups. The immobilization of DNA probe was based on the fact that the aldehyde group of GA could be attacked by primary amino groups of AET and DNA probes to form a covalent bond, which can be stabilized by a dehydration reaction and lead to Schiff base formation. Figure 1 provides an overview of the overall scheme of the covalent coupling of GA to AET-modified electrodes for the attachment of 5′-NH_2-modified oligonucleotide probes. The alkylamine group facilitates the

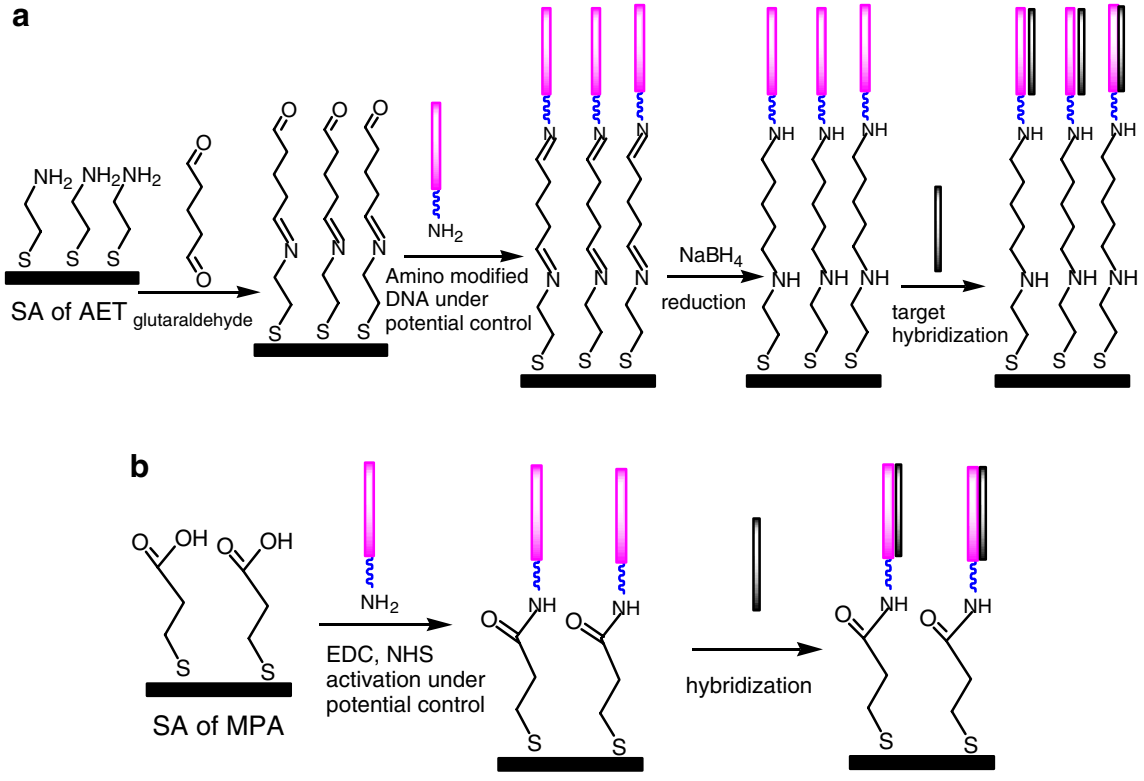

Fig. 1 Schematic illustration of the covalent coupling of 5-NH_2-modified oligonucleotides to AET-modified electrodes, with the coupling of GA (**a**) and MPA-modified electrode (**b**)

crosslinking of primary amines by activated GA. The Schiff base reaction is reversible at acidic pH. Consequently, the electrodes must be reduced with the addition of sodium borohydride ($NaBH_4$) for a valid immobilization of the probe. The pretreated electrodes were immersed into 1 mmol l^{-1} AET ethanol solution for 16 h, resulting in an AET assembly on the electrodes. After that, the electrodes were thoroughly washed with ethanol and distilled water. The electrode was kept in distilled water until use and was denoted as AET/Au. The covalent coupling of GA was accomplished by incubating the AET/Au electrode in 5% GA in 0.1 mol l^{-1} PBS (pH 7.4) at 37°C for 2 h, subsequently rinsing the electrode twice with PBS and deionized distilled water, followed by drying with nitrogen purge. The electrode was denoted as GAAET/Au. The potential control immobilization of the single-stranded (ss) DNA probe on aldehyde-functional GAAET/Au was conducted at the potential control as reported previously [20]. Briefly, fresh GA-functional electrodes were immersed into the electrochemical cell containing 2 μg ml^{-1} of complementary, one-base mismatch, and noncomplementary ss-DNA probe solutions, respectively, in PBS under the controlled potential of +0.2 V vs SCE for 0.5 h. After the controlled potential immobilization, the electrode was then incubated overnight in a humid chamber at a temperature of 37°C, followed by soaking for 5 min in 0.1% SDS and distilled water, respectively, to remove any nonspecifically absorbed DNA. The probe-modified electrodes were subsequently reduced with $NaBH_4$ for 30 min and rinsed with 0.1 mol l^{-1} PBS for 30 min, which were denoted as Comp-ss-DNAGAAET/Au, M1bcomp-ss-DNAGAAET/Au, and Mismatch-ss-DNAGAAET/Au, respectively.

ss-DNA probe immobilization on MPA-modified electrode

In the presence of a water-soluble carbodiimide regent, the 5′-terminal amino group of oligonucleotide probe formed an amide bond with the primary carboxyl group of MPA monolayer on the gold electrode surface [22]. The DNA can be covalently immobilized onto modified electrodes using EDC and NHS as activation coupling reagents. As shown in Fig. 1b, MPA-modified electrodes (denoted as MPA/Au) were initially immersed into an activation solution containing 5 mM EDC and 8 mM NHS in PBS (pH 7.0) for 15 min. These electrodes were subsequently used as working electrodes in the electrochemical cell containing 2 μg ml^{-1} of complementary, one-base mismatch, and noncomplementary ss-DNA probe solutions, respectively, in TE buffer under the controlled potential of +0.2 V vs SCE for 0.5 h. The other procedure for eliminating nonspecific ss-DNA is the same as in "Single-stranded DNA probe immobilization on GA-modified electrode." The ss-DNA probe-modified MPA electrodes were denoted as Comp-ss-DNAMPA/Au, M1bcomp-ss-DNAMPA/Au, and Mismatch-ss-DNAMPA/Au, respectively.

ss-DNA probe immobilization on microarray

The oligonucleotides probe were suspended in 1× microspotting solution (Telechem) up to a final concentration of 80 pmol μl^{-1}. Approximately 1 nl (0.05–0.1 pmol) of each oligonucleotide was printed in quadruplicate as microdots (100 μm in diameter) on superaldehyde-coated glass slides (DAKO) using a PixSys5500 microarray (Cartesian Technology). The arrays of spots were from left to right and from top to bottom (see Fig. 5). The slides were washed thoroughly with 0.1% SDS to remove any unbound oligonucleotides. After further treatment with a $NaBH_4$ solution for 30 min, the slides were ready for hybridization.

Hybridization reaction with the target ss-DNA

By immersing the ss-DNA probe-modified electrodes or the slides into a unihybridization solution (1:4 dilution, vol vol^{-1}; Telechem), the hybridization reactions were conducted in a moist hybridization chamber under a cover slip at 42°C for 2 h. Subsequently, these electrodes and slides were rinsed and washed with 2× SSC–0.1% SDS and 0.1× SSC–0.1% SDS, respectively, for a total of 15 min to remove any nonspecifically bound species. The electrodes were subsequently dried with nitrogen purge. The slides were dried by centrifugation at 500 rpm for 5 min. The fully complementary, one-base mismatched, and fully mismatched hybridized electrodes were denoted as Comp-ds-DNAGAAET/Au, M1bcomp-ds-DNAGAAET/Au, Mismatch-ds-DNAGAAET/Au, Comp-ds-DNAMPA/Au, M1bcomp-ds-DNAMPA/Au, and Mismatch-ds-DNAMPA/Au, respectively.

Regeneration of probe-modified electrodes and the microarray

The procedure was conducted by incubation of the hybridized electrodes and slides at 95°C for 5 min, followed by quick cooling in ice water and sequential rinsing with 0.1% SDS phosphate buffer (pH 7.4) and 2× SSC buffer to remove previously hybridized species. The regenerated electrodes and slides were reused for detecting the target of $p16^{INK4A}$ using the same procedure as in "Hybridization reaction with the target ss-DNA."

Image scanning and data processing

The microarray slide was scanned with the ScanArray Lite Microarray Analysis Systems (a Packard BioScience company, USA) after the above treatment. The images acquired by the scanner were analyzed with the software Genepix Pro 3.0. Each spot was defined by the positioning of a grid of circles over the array image. For each fluorescent image, the average pixel intensity within each circle was determined, and a local background using mean pixel intensity was computed for each spot. The net signal was determined

by a subtraction of this local background from the mean average intensity for each spot. Statistical analyses were conducted using the Origin 7.0 software.

Results and discussion

Specificity in the detection of one-base mismatch label-free target with CV

The DNA probes were assembled on the modified gold electrode based on GA and MPA coupling, respectively. To test whether the coupling of GA was sufficiently selective to distinguish a mismatch of only a single base pair, these electrodes were reacted with the target in the hybridization buffer, and the recognition of differently modified electrodes was carried out with CV using 0.12 mM $[Co(phen)_3](ClO_4)_3$ as a redox indicator that was added in the Tris–HCl buffer solution. Figure 2 shows comparisons of CV curves based on GA (a) and MPA (b) coupling, respectively, in the absence of DNA, Comp-ds-DNA, M1bcomp-ds-DNA, and Mismatch-ds-DNA at a scan rate of 50 mV s^{-1}. Figure 3 shows a comparison of anodic peak currents vs the root of the scan rate of CV $\upsilon^{1/2}$ based on GA coupling (a), respectively, of GAAET/Au, Comp-ds-DNAGAAET/Au, M1bcomp-ds-DNAGAAET/Au, and Mismatch-ds-DNAGAAET/Au, and based on MPA coupling (b) of MPA/Au, Comp-ds-DNAMPA/Au, M1bcomp-ds-DNAMPA/Au, and Mismatch-ds-DNAMPA/Au electrodes in Tris–HCl buffer (pH 7.1) containing 0.12 mM $[Co(phen)_3](ClO_4)_3$.

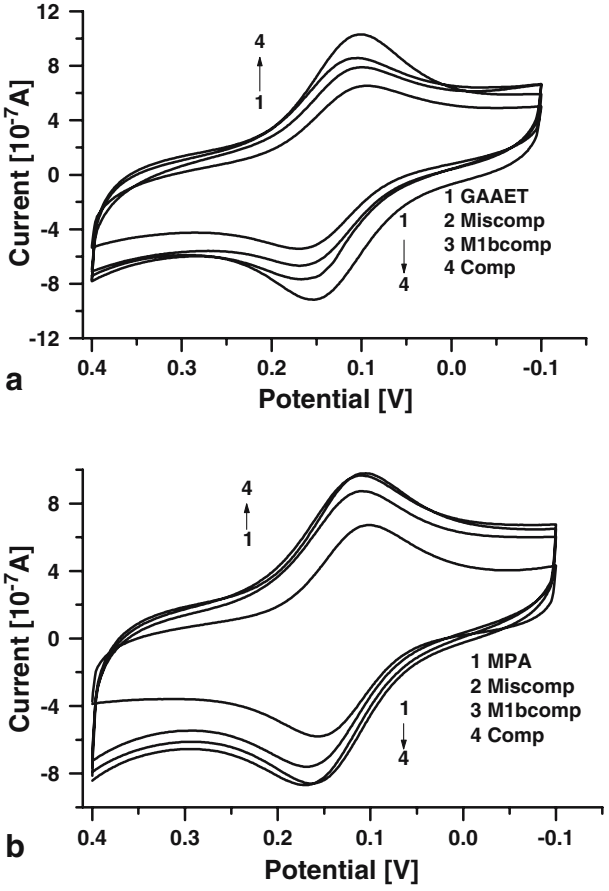

Fig. 2 Comparison of CV based on the GA coupling (**a**) of GAAET/Au, Comp-ds-DNAGAAET/Au, M1bcomp-ds-DNAGAAET/Au, and Mismatch-ds-DNAGAAET/Au, and on the MPA coupling (**b**) of MPA/Au, Comp-ds-DNAMPA/Au, M1bcomp-ds-DNAMPA/Au, and Mismatch-ds-DNAMPA/Au electrodes at a scan rate of 50 mV s^{-1} in a Tris–HCl buffer (pH 7.1) containing 0.12 mM $[Co(phen)_3](ClO_4)_3$

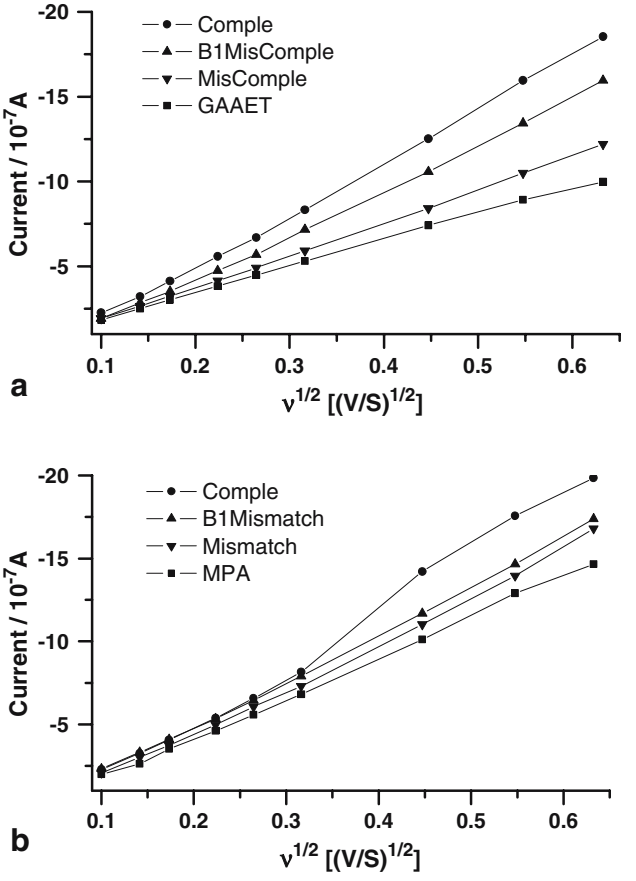

Fig. 3 Comparison of anodic peak currents vs the root of the scan rate of CV $\nu^{1/2}$ based on the GA coupling (**a**) of GAAET/Au, Comp-ds-DNAGAAET/Au, M1bcomp-ds-DNAGAAET/Au, and Mismatch-ds-DNAGAAET/Au, and on the MPA coupling (**b**) of MPA/Au, Comp-ds-DNAMPA/Au, M1bcomp-ds-DNAMPA/Au, and Mismatch-ds-DNAMPA/Au electrodes in a Tris–HCl buffer (pH 7.1) containing 0.12 mM $[Co(phen)_3](ClO_4)_3$

Comprehensively, the following features were observed:

(1) The redox peak currents of $Co(phen)_3^{3+}$ species reflected the hybridized status of the $p16^{INK4A}$ gene. Figure 2a shows that the anodic peak currents at the Comp-ds-DNAGAAET/Au electrodes [(6.3±0.5)×10^{-7} A] are much larger than those at M1bcomp-ds-DNAGAAET/Au [(4.5±0.5)×10^{-7} A], Mismatch-ds-DNAGAAET/Au [(3.6±0.4)×10^{-7} A], and bare GAAET/Au [(3.5±0.4)×10^{-7} A], whereas a significantly less difference of anodic peak currents [(5.6±0.5)×10^{-7} A] is observed at the Comp-ds-DNAMPA/Au electrode with respect to those obtained at M1bcomp-ds-DNAMPA/Au [(5.1±0.5)×10^{-7} A], Mis-

match-ds-DNAMPA/Au [(4.7±0.4)×10^{-7} A], and MPA-modified electrodes [(3.6±0.4)×10^{-7} A]. An adequate discrimination of an approximately eightfold signal difference between the complementary hybridized and mismatch hybridized electrodes, compared with a bare GAAET/Au electrode, was obtained based on GA coupling. Only a ~2.5-fold signal difference of that compared with the MPA-modified electrode was deduced based on MPA. Because the peak current intensity of mismatch-ds-DNAGAAET/Au (curve 2) was the smallest among the three electrodes, a complementary match threshold could be established [23]; therefore, the target gene could be determined. These data suggested that a good quality of the basis for immobilization of ss-DNA probes used to discern fully complementary, one-base mismatched, and noncomplementary hybridizations was formed by covalently coupling GA onto the AET modified gold electrode.

(2) In the case of the bare GAAET/Au electrode, the peak potential separation ($\Delta E_p = E_{pa} - E_{pc}$) was found to be between 60 and 70 mV, independent of potential sweep rate ($10 \le v \le 200$ mV s^{-1}), where ΔE_p, E_{pa}, and E_{pc} represented redox peak separation potential, anodic peak potential, and cathodic peak potential, respectively. These indicated that the reduction of $[Co(phen)_3]^{3+}$ at the surface of the electrode was a close, reversible one-electron redox process. A linear correlation between the anodic peak current and the square root of the scan rate $v^{1/2}$ was observed (Fig. 3), as expected for a diffusion-controlled electrochemical process. For all electrodes, $R \ge 0.999$ and $P \le 0.001$, respectively (from the linear fitting in Fig. 3). On the other hand, at the Comp-ds-DNAGAAET/Au electrode, the anodic peak current increased rapidly with the $v^{1/2}$ and kicked up when the scan rate was more than 0.1 V s^{-1} (Fig. 3b), validating the adsorption of the electroactive species occurring at the surface of the electrode.

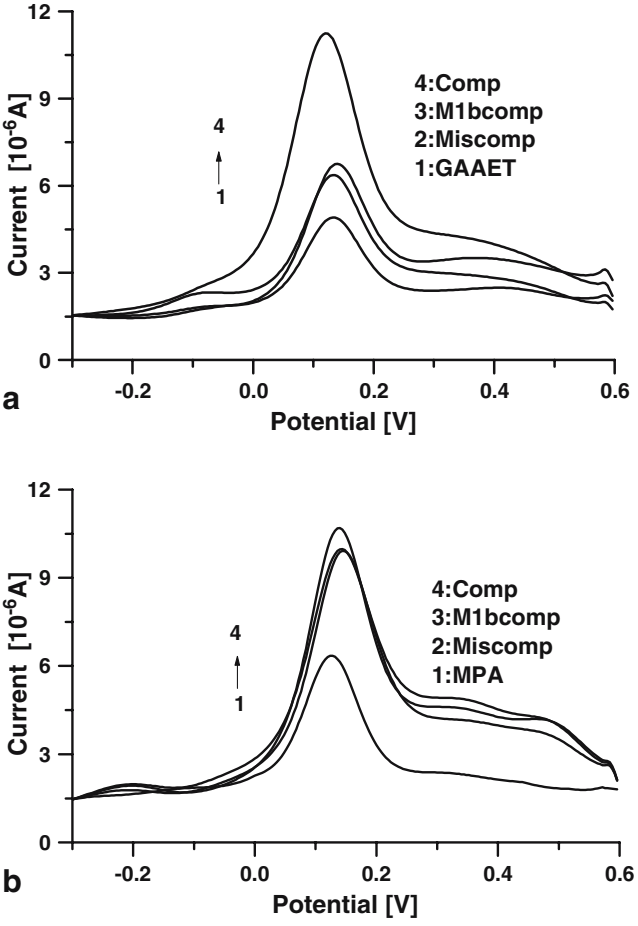

Fig. 4 Comparison of SWV based on the GA coupling (**a**) of GAAET/Au, Comp-ds-DNAGAAET/Au, M1bcomp-ds-DNAGAAET/Au, and Mismatch-ds-DNAGAAET/Au, and on the MPA coupling (**b**) of MPA/Au, Comp-ds-DNAMPA/Au, M1bcomp-ds-DNAMPA/Au, and Mismatch-ds-DNAMPA/Au electrodes with an amplitude of 25 mV, a pulse frequency of 30 Hz, and a step potential of 4 mV in a Tris–HCl buffer (pH 7.1) containing 0.12 mM $[Co(phen)_3](ClO_4)_3$

Discernment of one-base mismatch by SWV measurement for different electrodes

Square wave voltammetry, which combines an effective charging current compensation with a rapid scanning capability, is one of the most attractive modern pulse voltammetric methods and offers effective discrimination against background current, hence lowering the detection limits of voltammetric measurements [24]. The hybridized electrodes are also characterized with the SWV, and the cathodic peak currents of $Co(phen)_3^{3+}$ species are illustrated in Fig. 4. All current signals were subtracted from the background based on bare GA or MPA-modified electrodes. Based on the covalent coupling of GA, the cathodic peak current of $Co(phen)_3^{3+}$ species at the fully complementary DNA-modified electrode is as high as (6.37±0.23)×10^{-6} A (Fig. 4a, curve 4), which distinguishes the one-base mismatched [(3.35±0.24)×10^{-6} A, curve 3], fully mismatched [(3.15±0.21)×10^{-6} A, curve 2], and bare GA-modified electrodes [(2.45±0.21)×10^{-6} A, curve 1]. The peak potential of fully complementary DNA-modified electrode also shifts negatively (0.120 V) compared with that for single mismatched (0.140 V), fully mismatched (0.132 V), and bare GA-modified electrodes (0.130 V). Based on previous studies by Pang et al. [25] and Carter et al. [26], the shifts of peak potential are attributed to the interaction mode between the DNA and the redox indicator couples $[Co(phen)_3]^{3+/2+}$. The 2+ ion interacts more favorably via hydrophobic interaction with the DNA than does the 3+ ion. The potential shift in negative direction indicates that the DNA on the fully complementary DNA-modified electrode interacts electrostatically with the $[Co(phen)_3]^{3+/2+}$ vs that on the barely GA-modified electrode. This indicates that the redox indicator binds favorably to the duplex of the fully complementary DNA via electrostatic interactions. On the other hand, based on the MPA-modified electrode, the cathodic peak current of a fully complementary DNA-modified electrode is as high as (6.06±0.23)×10^{-6} A, which shows less difference from one-base mismatched [(5.50±0.29)×10^{-6} A], fully mis-

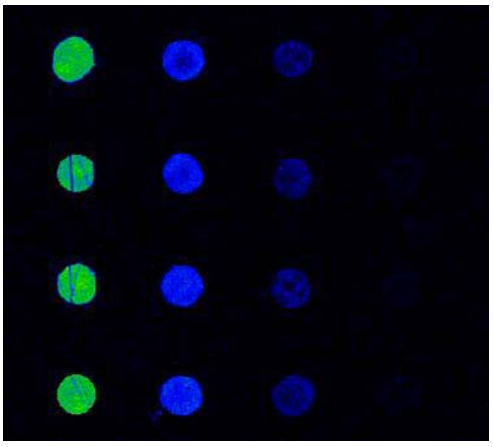

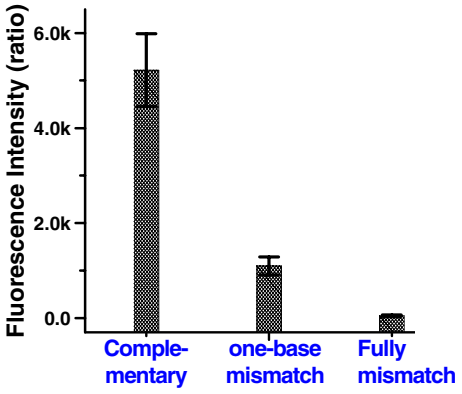

Fig. 5 A fluorescent image (*left*) and a comparison (*right*) of the fluorescence intensity of surface-bound DNA after hybridization with the oligonucleotide target on the superaldehyde-coated glass. Fluorescence measurements (*black, high intensity*) of hybridization with a fluorescently labeled oligonucleotide target. The arrays of spots from *left* to *right* were perfectly complementary, one-base mismatched, and fully mismatched, respectively. Error bars reflect error estimates from measurements on four replicate samples

matched [(4.99±0.31)×10^{-6} A], and bare MPA-modified electrodes [(3.87±0.27)×10^{-6} A]. The ratios of cathodic peak current for a fully mismatched hybridized electrode to that for one-base mismatch on the coupling of GA and MPA, respectively, are about 1.90 and 1.10. The result also shows more difference in peak currents and potentials without labeling based on the GA-modified electrode, which coincides with the result of CV.

Microarray measurement for hybridization on superaldehyde-coated glass

The coupling of GA was also evaluated using the microarray technology. Fluorescence measurements of the hybridization of surface-bound DNA with fluorescently labeled target oligonucleotides in GA coupling are shown in Fig. 5, reflecting the fluorescence intensity of each spot. The intensity of fully complementary, one-base mismatched, and fully mismatched oligomer hybridizations was calculated, respectively, and averaged for three parallel experiments. The intensity of perfectly complementary hybridization was the greatest in all spots (as high as 5,218.8, with a standard deviation of 764.7) because of its perfectly complementary matching with oligonucleotides. However, one-base mismatch showed a greater intensity (1,098.9, with a standard deviation of 187.4) due to its interaction with the probe. Completely mismatched spots (48.5, with a standard deviation of 13.5) were the weakest. A quantitative analysis of fluorescence intensities further illustrates a feasible detection of hybridization based on GA coupling.

Surface stability toward multiple hybridization denaturation cycles

To test the stability and accessibility of the surface, we performed experiments in which the probe-modified electrodes were successively hybridized and denatured for four times. In each cycle, the probe-modified electrode was hybridized with the target, and the anodic peak currents of CV for different electrodes were measured at a scan rate of 100 mV s^{-1}. The DNA-duplex-modified electrode was then denatured, followed by rinsing with water. This procedure will rejuvenate the probe-modified electrode. Figure 6 shows the anodic peak currents of CV for different electrodes during each hybridization cycle. The response of CV was very stable, and approximately 85% of the initial activity was still maintained after four cycles of denaturation. The discrimination between perfectly complementary and one-base mismatch hybridizations is clear within the same regeneration time. The decreases in signal with time were probably due to the breakdown of the probe during heating denaturation. The result indicates that the probe-modified GA coupling electrodes can be reproduced to hybridize the multiple detection of targets to make additional measurements with a regeneration time label.

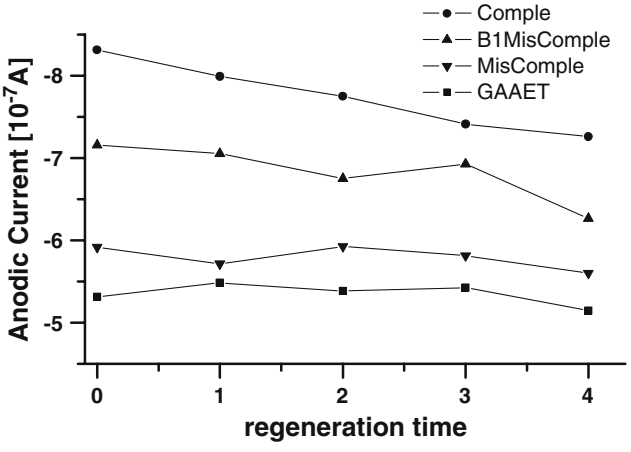

Fig. 6 Comparison of anodic peak currents of SWV for different electrodes vs multiple hybridization and denaturation cycles. The scan rate is 100 mV s^{-1} and the measurement condition is the same as that in Fig. 2

Although the concentration of the target is fixed in the present research, a one-base mismatch of expression profiles is able to be detected from small amounts of tissues through the amplification of DNA populations with the help of PCR. The amount of the sample target in the present study has been obtained from gastric tumor tissues in our work [27]. This may prove effective in the discrimination of one-base mismatches in voltammetric detection measurements for different electrodes.

Interpretation of GA on the improvement of discrimination of one-base mismatch

The helix formation of DNA immobilization can take place only in those cases where the points of fixation are arranged in appropriate distances to each other. A covalent attachment of hetero/homobifunctional and trifunctional cross-linkers facilitates the coupling of ligands with unusually available chemical groups. A covalent introduction of a spacer arm GA permits a secure but flexible attachment of many different molecules. Coupling with GA results in the DNA probe being bound 11–12 carbon atoms away from the surface of the electrode vs two to three carbon atoms as in the case of a carboxylate electrode coupled using carbodiimide. The sterical reason seems to be responsible for the dramatic difference in the discrimination of one-base mismatch, as Bünemann et al. [28] reported for 1,4-butanediol diglycidyl ether. The accessibility of DNA immobilization has been shown to depend more crucially on the method of immobilization than on the type of support used for fixation. The fixation of DNA via longer spacers (GA) generated detectable mismatches under suitable activation conditions, indicating a simple correlation between the mismatch and the basis of immobilization, where the linker does not prevent hydrogen bonding and stacking of bases involved in the linkage. The thickness of GA-functional layers may help to minimize nonspecific adsorption by reducing the possibility of entanglement of DNA molecules coupling with our potential control assembly. The GA could be indebted to the improvement of steric hindrance and may limit close proximity, showing a better overall accessibility than that of MPA as long as DNA fragments with suitable sizes are used. Generally, the GA that served as the arm molecule can be correlated with the enhancement of mismatch effect, the improvement in the yields of coupling, and a reduced accessibility of immobilized DNA. The ss-DNA in the coupling medium forms more or less random coils and is fixed as such. With an increase in linkages between DNA strands and the supporting bases, the chance for the formation of favorably spaced points of attachment with respect to the helix structure, to be formed in the course of hybridization later on, increases dramatically. Longer spacers could gradually improve spatial requirements for hydrogen bonding and helix formation, as can be seen above. Otherwise, they are not sufficiently extended for an efficient compensation of steric restrictions caused by unfavorably spaced fixation points. The coupling medium may somehow prevent the formation of linkages that are unfavorable for helix formation in the course of hybridization.

GA can be advantageous for DNA hybridization instead of commonly used solid materials. The favorable qualities essentially result from the combination of high yields of coupling reaction and the total accessibility of DNA immobilization. This difference may be caused by the fixation of DNA on the surface of solid materials, instead of the network-like structures of GA.

Conclusion

This work demonstrates that the chemistry described here is sufficient to specifically identify a single-base mismatch with excellent discrimination. GA can be used as a coupling substrate for DNA immobilization with good sensitivity, selectivity, and reversibility. The level of nonspecific adsorption on these GA surfaces is sufficiently low such that one can clearly distinguish mismatches of only one base pair using CV and SWV measurements. Due to the simplicity, flexibility, and practicality of this method, its wide applications in the development of future nanoelectronic devices and electrochemistry studies is expected. The method reported here provides an avenue for the development of devices in which the exquisite binding specificity of biomolecular recognition is directly coupled to devices.

Acknowledgements This work was supported by the National Natural Science Foundation of China (grant nos. 90406023, 60371027, 60121101) and the Natural Science Foundation of Jiangsu (China; grant nos. 03KJD310177 and JHB04-005).

References

1. Serrano M, Hannon GJ, Beach D (1993) Nature 366:704–707
2. Cody DT II, Huang Y, Darby CJ, Johnson GK, Domann FE (1999) Oral Oncol 35:516–522
3. Bickle TA, Kruger DH (1993) Microbiol Rev 57:434–450
4. Frommer M, McDonald LE, Millar DS, Collis CM, Watt F, Grigg GW, Molloy PL, Paul CL (1992) Proc Natl Acad Sci U S A 89:1827–1831
5. Kane MF, Loda M, Gaida GM, Lipman J, Misbra R, Goldman H, Jessup JM, Kolodner R (1997) Cancer Res 57:808–811
6. Herman JG, Graff JR, Myöhänen S, Nelkin BD, Baylin SB (1996) Proc Natl Acad Sci U S A 93:9821–9826
7. Kuppuswamy MN, Hoffmann JW, Kasper CK, Spitzer SG, Groce SL, Bajaj SP (1991) Proc Natl Acad Sci U S A 88:1143–1147
8. Adorján P, Distler J, Lipscher E, Model F, Műller J, Pelet C, Braun A, Florl AR, Gűtig D, Grabs G, Howe A, Kursar M, Lesche R, Leu E, Lewin A, Maier S, Műller V, Otto T, Scholz C, Schulz WA, Seifert HH, Schwope I, Ziebarth H, Berlin K, Pipenbrock C, Olek A (2002) Nucleic Acids Res 30:e21
9. Hou P, Ji MJ, Liu ZC, Shen JY, Cheng L, He NY, Lu ZH (2003) Clin Biochem 36:197–202
10. Pennisi E (1999) Science 283:1822–1823
11. Wang J, Xu D, Kawde A, Polsky R (2001) Anal Chem 73:5576–5581
12. Lee T, Shim YB (2001) Anal Chem 73:5629–5632
13. Boon EM, Ceres DM, Drummond TG, Hill MG, Barton JK (2000) Nat Biotechnol 18:1096–1100

14. Takenaka S, Yamashita K, Takagi M, Uto Y, Kondo H (2000) Anal Chem 72:1334–1341
15. Peña SRN, Raina S, Goodrich GP, Fedoroff NV, Keating CD (2002) J Am Chem Soc 124:7314–7323
16. Herne TM, Tarlov MJ (1997) J Am Chem Soc 119:8916–8920
17. Satjapipat M, Sanedrin R, Zhou F (2001) Langmuir 17:7637–7644
18. Takenaka S, Yamashita K, Takagi M, Uto Y, Kondo H (2000) Anal Chem 72:1334–1341
19. Ausubel FM, Brent R, Kingston RE, Moore DD, Seidman JG, Smith JA, Struhl K (1992) Short protocols in molecular biology. Wiley, New York, Unit 2.1
20. Ge CW, Liao JH, Yu W, Gu N (2003) Biosens Bioelectron 18:53–58
21. Dollimore LS, Gillard RD (1973) J Chem Soc Dalton Trans 933–940
22. Zhao Y, Pang D, Hu S, Wang ZL, Cheng JK, Dai HP (1999) Talanta 49:751–756
23. Wojciechowski M, Sundseth R, Moreno M, Henkens R (1999) Clin Chem 45:1690–1693
24. Barker GC, Gardner AW (1992) Analyst 117:1811–1828
25. Pang DW, Abruňa HD (1998) Anal Chem 70:3162–3169
26. Carter MT, Rodriguez M, Bard AJ (1989) J Am Chem Soc 111:8901–8911
27. Hou P, Ji MJ, Ge CW, Shen JY, Li S, He NY, Lu ZH (2003) Nucleic Acids Res 31(16):e92
28. Bünemann H, Westhoff P, Herrmann RG (1982) Nucleic Acids Res 10:7163–7180